

The First Italian Experience of Ground Thermal Energy Storage: an Integrated Approach for Design and Monitoring, from Laboratory to Field Scale

Nicolò Giordano¹, Cesare Comina^{1,2} and Giuseppe Mandrone^{1,2}

¹Torino University, Earth Science Department, Via Valperga Caluso, 35 – 10125 Torino (IT)

²AG3 srl, Spin Off Company of Torino University, Via Valperga Caluso, 35 – 10125 Torino (IT)

nicolo.giordano@unito.it

Keywords: ground storage, analogical modeling, numerical modeling, geophysical monitoring, Italy

ABSTRACT

The ground thermal energy storage (GTES) is a useful application able to provide the H&C and DHW demand of commercial or residential buildings. Several examples in Canada and Northern Europe demonstrated the reliability and convenience of these systems in terms of both energy and economic savings, even though a remarkable initial investment is required. Owing to these conspicuous costs, an accurate preliminary study should be undertaken in order to correctly design the plant and achieve good efficiency of the system. Moreover, when the plant is operative, the monitoring of the thermal plume induced in the undisturbed ground should be a priority. The surrounding litho, hydro and biosphere are indeed influenced by the plant's activity and a trustworthy supervision of the temperature field is advisable both for the environmental safety and for controlling the system's efficiency. For these purposes, an integrated approach for design and monitoring GTES systems was tested first at laboratory scale and then applied to a field scale living lab, located nearby Torino (Northern Italy). The proposed methodology consists in lab analogical modeling of the heat propagation, geophysical measurements exploiting the existing relationship between temperature and electrical resistivity and numerical simulations of the studied phenomena with an open-source software (OpenGeoSys). The joint effort of temperature monitoring and numerical simulation at both lab and site scale, combined with direct measurements of the thermal properties, can be a useful tool for highlighting the best design solution for a GTES system. Moreover electrical resistivity surveys, calibrated at lab scale and then conducted at field scale, can be very useful in imaging the Thermal Affected Zone generated by the plant. The adopted approach showed a good potential towards reliable design and accurate monitoring activity.

1. INTRODUCTION

The thermal energy storage is a highly debated concept which was first mentioned in the late 1970s, when the energy crisis related to the high cost of fossil resources leaded the oil-dependent countries to think about alternative ways of energy production. The idea of exploiting the energy provided by renewable sources has been always accompanied by the problem that most of these sources can supply energy when the user's demand is low (e.g. most of the sun energy is related to the warm season, when the heating demand is reduced). In the recent years several storage technologies have been developed in order to find some valid solutions which can assure criteria of reliability, efficiency and economic sustainability. Short-term and long-term storage are the two big categories which discriminate the energy storage mechanism, depending on the daily or seasonal duration of the storing activity. The seasonal thermal energy storage seems to satisfy the annual heat demand better than the short-term, with a 60% of total energy demand against a 20% provided by the diurnal pattern (Fisch et al., 1998; Sanner, 2003; Xu et al., 2013). It is however true that the seasonal storage implies bigger economical investments and wider storage volumes, hence it results in a more challenging technology in terms of storing materials, heat loss evaluations and environmental impact reductions.

Three main categories of storage mechanism can be discerned: (i) sensible heat, (ii) latent heat and (iii) chemical reaction/thermochemical sorption heat. The first is considered to be a simple, low-cost, more reliable and acceptable technology compared to other alternatives, even if the latter methods have higher energy storage densities (more detailed discussion can be found in Xu et al., 2013). The underground thermal energy storage (UTES) system is a sensible heat based technology and includes several methodologies for storing the heat: exploiting the groundwater (ATES – aquifer thermal energy storage) (Paskoy et al., 2000; Dickinson et al., 2009), hot water confined in steel tanks (Novo et al., 2010; Schmidt et al., 2004) or the ground itself, being it constituted by rocks or saturated/partially saturated sediments. In the last case the connection with the ground is provided by a series of borehole heat exchangers (BTES – borehole thermal energy storage) (Fisch et al., 1998; Reuss et al., 2006; DLSC, 2012).

Mainly ATES and BTES have therefore geological implications. The thermal and hydrogeological properties of the ground have indeed to be taken into account not only in the design stage of the plant, but also after the plant's start up. Both ATES and BTES have a strong environmental impact; a big part of the aquifer is influenced in the first case, a noticeable underground volume is interested by drilling activity in the latter. In any case a not negligible thermal affected zone (TAZ) is generated and an accurate monitoring activity has to be considered to take care of the possible negative effects induced in the litho-, hydro- and bio-sphere.

So far, there is limited specific knowledge about the effects of unsuitable system design or the effects of groundwater temperature and chemical changes within the subsurface and the resulting consequences. A few studies have already measured the thermal effects of low enthalpy geothermal applications within field sites. Arslan and Huber (2013) compared their field temperature observations with numerical simulations and laboratory measurements under a forced groundwater flow. Lo Russo et al. (2014) focused on the thermal plume generated by the well doublets of the groundwater heat pumps, stressing the fact that the plumes may be regarded either as a potential anthropogenic geothermal resource or as a pollution. Bonte (2013) studied the temperature-induced impacts on the groundwater quality, taking into account the effects on the mobility of trace elements, the redox processes and the effects on microbial communities. Most studies agree that a 10°C temperature change can be sufficient to stimulate trace elements mobility and microbial activity variations. In general, by considering the high temperature (60°C – 70°C) injected in the ground by

BTES or ATES in order to generate a later exploitable thermal source, this could reflect in a relevant environmental impact which cannot be neglected.

The present study aims therefore to carry out an integrated and multidisciplinary approach for both the design and the monitoring of thermal energy storage systems. In this respect a laboratory device was built for simulate at small scale a heat injection comparable to the one that common BTES plants induce in the ground. Several tests were performed in different natural materials in order to describe the heat propagation by changing a number of key factors such as water content, position and number of the heat sources, water flow velocity and grain size distribution. On such a device, electrical resistivity measurements were moreover tested and calibrated together with devoted numerical simulations of the induced heat fluxes. Moreover, a BTES living lab was later developed in Grugliasco (Torino, Italy), consisting in 4 borehole heat exchangers (BHEs) coupled with 2 solar thermal panels. This plant represents an experimental site at field scale, which allows performing tests similar to those carried out at lab scale. Continuous temperature monitoring, periodical geophysical surveys and calibrated numerical simulations have therefore been implemented since the plant was launched at the beginning of spring 2014.

In the following, the outcomes of laboratory tests focused on a gravelly sandy medium, similar to the natural sediments founded in the Grugliasco site, are presented. A heat injection simulation with temperature monitoring, numerical modeling and geophysical surveying at lab scale were performed as a potential field scale approach. Preliminary results from the BTES living lab are moreover showed. It is in the authors' opinion that the whole methodology has potential to be undertaken for the ground's thermal behavior assessment, towards a reliable design and a trustworthy monitoring activity, which is very often underestimated.

2. THEORETICAL BACKGROUND

2.1 Numerical modeling

Numerical modeling has become a useful, maybe fundamental, tool in different disciplines, above all in those involving the ground and its interactions with anthropic applications. As far as the geothermal sector is concerned, the ability in predicting, by numerical methods, the productivity of deep high enthalpy reservoirs is nowadays a big part of the exploration activity, in which data from experimental and field tests converge to generate reliable 2D or 3D models of the underground. At the same time, the chance to describe the distribution of the thermal plume induced by shallow geothermal applications has revealed to be helpful both in the design stage and in the essential monitoring activity. Given the different dimensions of the plants and the economic effort in respect to high enthalpy systems, devoted field testing or proper parameter calibrations are however rarely undertaken. Analogical modeling and field tests have conversely to be the starting step of whatever preliminary study.

Several numerical codes have been developed during the past decades (Anderson, 2005; Hecht-Méndez et al., 2010); all of them are based on more or less the same governing equations. These can be summarized in the energy balance equation, taking into account each element of the three-component medium (solid, air and water):

$$\gamma_b C_b \frac{\partial T}{\partial t} + \nabla q_T = Q_T \quad (1)$$

where at the first member the temperature (T) variation in function of time (t) multiplied by density (γ_b) and specific heat capacity (C_b) of the medium are summed to the heat flux term (q_T). The latter can be divided in the two components of advective and conductive flux as follows:

$$q_T = \phi \theta \gamma_w C_w v T - \lambda_b \nabla T \quad (2)$$

where ϕ is the porosity, θ the water content, γ_w and C_w the density and the specific heat capacity of water, v denotes Darcy velocity and λ_b is the bulk thermal conductivity.

2.2 Electrical Surveys for Monitoring the Heat Propagation

Classic thermal tests or monitoring strategies often rely on local and point-based measurements to monitor changes in temperature. In this context, geophysics can bring complementary information which is spatially distributed and acquired directly from the ground surface. In particular, electrical resistivity measurements could be considered as a time and cost-efficient method for the long-term monitoring of the shallow geothermal systems.

Useful relationships can indeed be found in literature between temperature and electrical resistivity itself and can be potentially applied to monitor shallow geothermal applications. However resistivity depends in a complex way on different soil and environmental attributes. Friedman (2005) gave an overview of these parameters and their impact underlining three categories: (i) parameters describing the bulk soil, such as porosity (ϕ), water content (θ) and structure; (ii) the time-invariable solid particle quantifiers, such as particle shape and orientation, particle-size distribution, wettability or cation exchange capacity (CEC); (iii) fast-changing environmental factors, such as ionic strength, cation composition and, finally, temperature. On site a proper, but not easy, parameter calibration should be undertaken in order to infer relevant information such as the extension of TAZ. Devoted tests are therefore necessary in this respect. Laboratory tests have the advantage that controlled boundary conditions can be obtained (parameters from the first and the second group) such that a direct comparison of geophysical results, direct temperature measurements and numerical simulations can be performed. It is then possible to use the electric resistivity variations as a recording factor for imaging the time-lapse temperature distribution.

Hermans et al. (2012) demonstrated the ability of ERT to study heat flow and heat storage within a small field experiment in a shallow aquifer. They injected heated water and monitored the electrical resistivity values with cross-borehole time-lapse ERT. Fragkogiannis et al. (2008) also used ERT for monitoring the thermal performance of the ground at the University of Athens with an installed ground source heat pump (GSHP) system consisting of 12 BHEs. Robert et al. (2013) under laboratory conditions

highlighted the problems of ERT-derived temperatures owing to chemical reactions occurring within the underground, both on fluid and solid phases. They observed a divergence between the resistivity and temperature curves related to the increasing solubility of some minerals and the increasing fluid conductivity with increasing temperature.

3. LABORATORY SCALE

3.1 Materials and Methods

3.1.1 Laboratory Device

A plastic box, sized 1.0 x 0.4 x 0.4 m, was prepared to simulate a heat injection within the selected porous medium (Figure 1). Three sectors separated by permeable septa were predisposed in order to focus the simulation in the central part of the box. In the external sectors two PVC pipes surrounded by a high porosity filling material were placed for generating a water flow by controlling the hydraulic head in the external pipes. The central sector, about 0.6 m long, was filled with a porous medium for 0.3 m of thickness and was equipped with 4 thermo-resistances Pt100 (accuracy $\pm 1^\circ\text{C}$, resolution 0.2 $^\circ\text{C}$) for the temperature monitoring and with 4 Watermark soil moisture sensors (accuracy $\pm 1^\circ\text{C}$, resolution 0.2 $^\circ\text{C}$) previously properly calibrated, in order to check simultaneously the moisture conditions. Two electrical resistances (diameter 4 cm) powered by alternated current were used as a heat injection source. During the tests, the sources were controlled by a thermometer and a rheostat to assure the desired constant temperature. The boundaries of the box were thermally insulated by means of cork panels and impermeable membranes. A data logger and appropriate software were used for data acquisition in order to continuously register all the controlling parameters (sampling interval 1 minute). The porous medium adopted for the experiments here presented was a coarse medium with 58% vol. of gravel (mean particle diameter $d_0 = 5\text{--}6\text{ mm}$) and 42% vol. of sand, compacted at a porosity of 0.35. These conditions are approximately similar to those of the field test. In order to evaluate the variability of the thermal behavior as a function of water content, several experiments were performed: examples from $\theta = 0, 50, 100\text{ \% vol.}$ are here presented. Moreover, tests with flowing water were carried out by inducing a hydraulic head gap between the two side of the box. A flow rate of about $3.0 \times 10^{-3}\text{ l/s}$ of tap water at room temperature was provided.

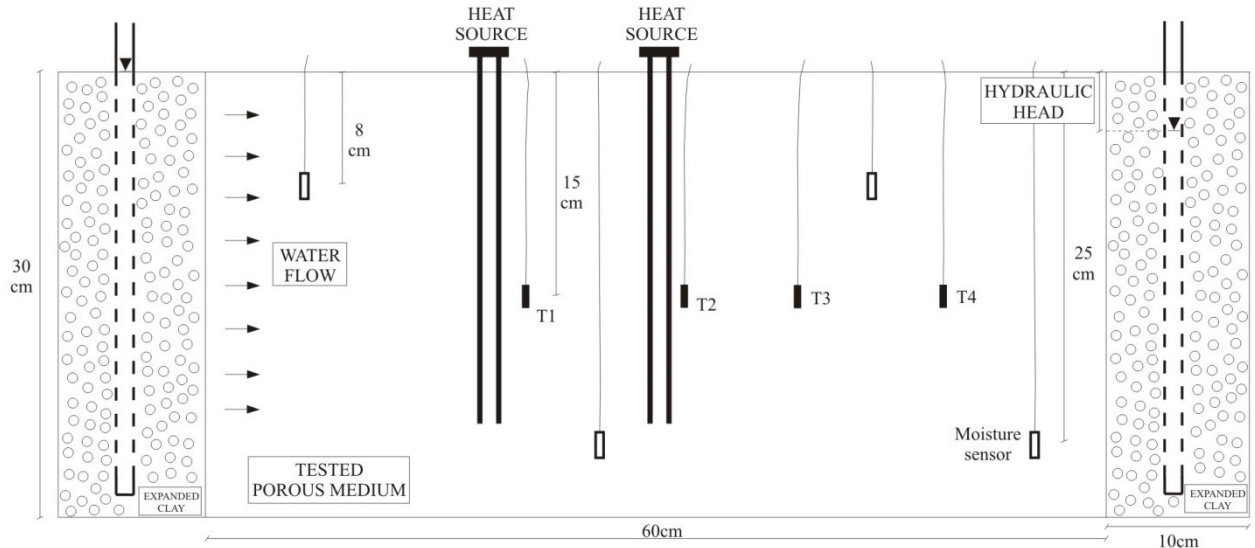


Figure 1: 2D sketch of the laboratory device used for the heat injection analogical modeling.

In parallel to the analogical modeling, a quantitative assessment of the thermal properties was carried out. The thermal conductivity was measured with the device ISOMET 2114 (Applied Precision, Ltd., Bratislava, Slovakia), which is based on the Transient Plane Source Method: a known current is applied to the sensor's heating element providing a small amount of heat (typically less than 2 $^\circ\text{C}$). Hence, the recorded voltage drop at the sensor element is used to determine the thermal conductivity of the tested medium. The device measures in a $0\text{--}6\text{ W m}^{-1}\text{ K}^{-1}$ range with a 5% accuracy. With this approach thermal conductivity values in dry and wet conditions were obtained; the $\theta = 50\text{ \% vol.}$ value was calculated with the Chen (2008) model. The volumetric heat capacity was evaluated by applying a classical formula (Campbell and Normann, 1998):

$$Cv = \gamma_w C_w \Phi \theta + \gamma_a C_a \Phi (1 - \theta) + \gamma_s C_s (1 - \Phi) \quad (3)$$

where γ_w , γ_a and γ_s are the density of water, air and solid (1.0×10^3 , 1.0 and $2.73 \times 10^3\text{ kg m}^{-3}$ respectively), C_w , C_a and C_s are the specific heat capacity of water, air and solid (4.19 , 1.01 and $0.76\text{ kJ kg}^{-1}\text{ K}^{-1}$ respectively), ϕ and θ are the porosity and the water content. The thermal diffusivity is typically known as the ratio between conductivity and volumetric heat capacity as follows (Farouki, 1981):

$$\alpha = \frac{\lambda}{Cv} \quad (4)$$

3.1.2 Numerical simulations

In order to valuably define the temperature distribution within the box, a numerical simulation with the OpenGeoSys code (Kolditz et al., 2012) was performed. OpenGeoSys (OGS) is an open-source initiative for the numerical simulation of thermo-hydro-

mechanical/chemical processes (THM/C). It is a flexible numerical framework based on the Finite Element Method (FEM), provided to solve multifield problems in porous and fractured media for several geological and hydrological applications. The simulations were performed using the *heat_transport* process for the static tests and the coupled *heat_transport* and *groundwater_flow* processes for the tests simulating coupled conduction and advection phenomena. Some preliminary evaluations were carried out by comparing *ad hoc* simulations with available analytical solutions and experimental tests. With this aim geometric elements, discretization mesh, Dirichlet and Neumann boundary conditions, time step definition, medium, material and fluid properties were calibrated. The numerical modelling was carried out by setting up the same characteristics of each experimental test performed at lab scale. A 3D model with a rectangular prismatic mesh of about 75,000 nodes was adopted. The lateral sides of the box were simulated as impermeable boundaries, not allowing for heat or fluid flow (except for the water flow tests) and only the upper boundary was a diffusing one. The finally adopted physical properties of the tested material are presented in Table 1. The simulated tests lasted 10 hours (5 h for heat injection and 5 h for the medium's cool down) divided in 20 steps of 0,5 hours each one. The simulations were performed on a computer equipped with an Intel® Core™ i5-3317U 1.70 GHz CPU processor with 4.00 GB of RAM and the 64-bit Microsoft Windows 8® operating system.

ϕ	γ_b [$t\ m^{-3}$]	k_i [m^2]	λ_s [$W\ m^{-1}\ K^1$]	λ_w [$W\ m^{-1}\ K^1$]	C_s [$kJ\ kg^{-1}\ K^1$]	C_w [$kJ\ kg^{-1}\ K^1$]	Δi [m]	
Tested medium	0.35	1.72	$3.00\ 10^{-11}$	5.00	0.58	0.76	4.19	0.05

Table 1: Physical properties of the tested medium adopted for OGS numerical simulations. From the left there are porosity, bulk density, permeability coefficient, thermal conductivity of solid and water, specific heat capacity of solid and water, hydraulic head gap.

3.1.3 Geophysical Surveys

A geophysical monitoring of the temperature distribution was performed. By exploiting the general relationship which links electrical resistivity with temperature, electrical surveys during both the heating and the cooling period of the tests were carried out. The experiment here presented was performed on the medium at $\theta = 100\ %$ vol., without water flow. A network configuration with 24 electrodes (6 lines of 9 cm spaced electrodes) was adopted to achieve a wide spatial information around the sources (Figure 2). A SYSCAL Pro multichannel georesistivimeter was used for the resistivity measurements. A short current injection time (250 ms) was adopted in order to record the set of measurements as quick as possible. To ensure a reliable lateral coverage a Dipole-Dipole array with 36 measurements (plus reciprocal, for a total of 72 measurements) was adopted.

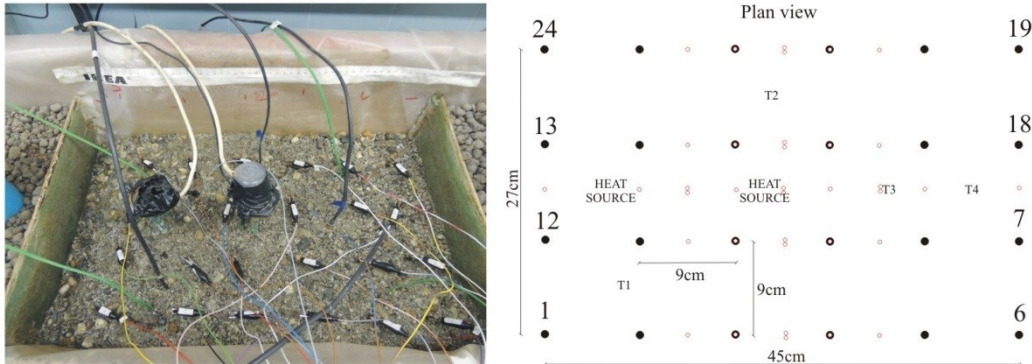


Figure 2: Electrode configuration adopted on the laboratory device for the heat injection monitoring. Black dots outline the 24 electrodes, red dots highlight the midpoints of the Dipole-Dipole measurements.

This described configuration allowed to record resistivity values roughly at the same depth of temperature sensors and to image resistivity variation during time in a plan view around the heat source. The electrical surveys were performed hourly from the beginning (zero condition) until the end of the test, when the undisturbed temperature was reached again. The applied methodology consisted in predicting the temperature distribution by analyzing the electrical resistivity difference among each step. A linear dependence between temperature and electrical conductivity (σ – the inverse of resistivity) is known under few tens of degrees °C. Around 25 °C the following relation has been proposed:

$$\frac{\sigma_T}{\sigma_{25}} = m(T - 25) + 1 \quad (5)$$

where σ_T is the electric conductivity of the porous medium at temperature T and m is the fractional change. Values ranging from $0.018\ ^\circ\text{C}^{-1}$ to $0.025\ ^\circ\text{C}^{-1}$ have been found by several authors for m (Revil et al., 1998; Hayashi, 2004; Hayley et al., 2007; Hermans et al., 2012) and they vary according to the type of fluid and sediments. From Equation [5], a formula customized for predicting the temperature distribution was adopted:

$$T_t = \frac{1}{m} \left(\frac{100}{\Delta\rho(\%)} - 1 \right) + T_0 \quad (6)$$

where $\Delta\rho(\%)$ is the percentage resistivity variation, T_t and T_0 are temperature values at time t and zero. Each electrical resistivity measurement was therefore subtracted to the zero condition and the amount of variation $\Delta\rho(\%)$ provided the temperature distribution within the medium.

3.2 Analogical Modeling: Results and Discussion

The analogical modeling provided an interesting qualitative evaluation of the heat propagation within the porous medium at changing water content. A temperature peak at intermediate water content was registered at each sensor in the static conditions (Figure 3). When the water flow was induced, the thermal propagation of the injected heat was clearly shifted downline of the sources and the Pt-100s placed downstream recorded the highest temperatures and the most elevated thermal gradients. The advection raised the effective thermal conductivity and also tended to equilibrate the temperature distribution throughout the medium. Indeed, nearby the sources (T1 and T2) the maximum temperature is reached by $\theta = 50$ % vol., while the further sensors (T3 and T4) recorded the highest peaks with the flowing water. On the other hand the advection managed to rapidly cool down the medium after the source's turn off, because the water at room temperature (18 °C) could easily lower the temperature field provided by the heat injection.

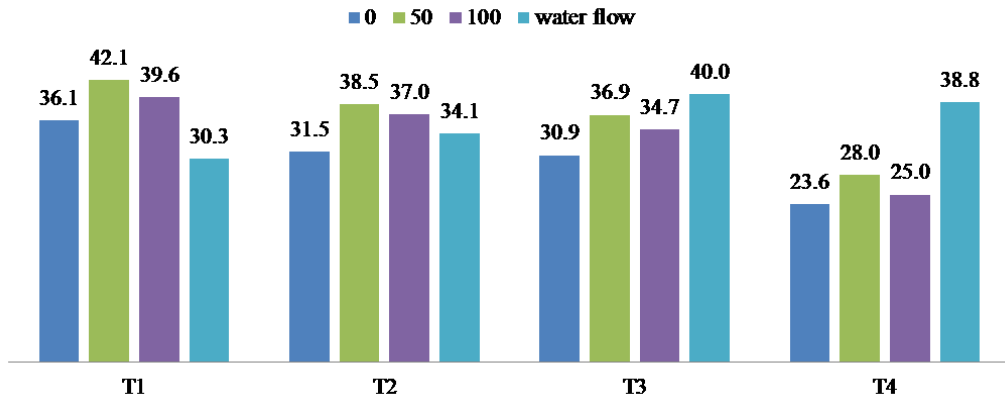


Figure 3: Temperature values recorded by each sensor at different water contents.

The measured and calculated thermal conductivities presented increasing values with an increasing water content as many literature data showed (Abu-Hamdeh and Reeder, 2000; Tarnawski and Leong, 2000; Ochsner et al., 2001; Chen, 2008). These values provided to achieve a thermal diffusivity trend with a peak at an intermediate water content (Table 2). This observation is therefore in accordance with the analogical simulation performed and with the qualitative evaluations above reported. The conductivity and diffusivity of the medium in the flowing water conditions are not measurable and difficult to calculate. An example reported in Comina et al. (2013) showed as the advection contributes at least for 50 % to the heat propagation, redoubling the effective thermal conductivity.

	Water content [%]		
	0	50	100
Thermal conductivity [$\text{W m}^{-1} \text{K}^{-1}$]	0.41 ± 0.03	1.65 ± 0.03	2.01 ± 0.05
Thermal diffusivity [$10^{-6} \text{m}^2 \text{s}^{-1}$]	0.32 ± 0.03	0.83 ± 0.03	0.73 ± 0.05

Table 2: Thermal properties of the tested medium at different water contents. The conductivity was measured with the ISOMET 2114 and calculated with the Chen (2008) model, the diffusivity calculated from the volumetric heat capacity.

In the perspective of a field application, the laboratory outcomes can be briefly summarized as follows.

- In the examined medium the maximum temperatures were observed at $\theta = 50$ % vol., when only conduction occurred. This is confirmed by the thermal diffusivity which is higher with the intermediate amount of water. Nevertheless, this strongly depends on the grain size distribution: in a finer medium, a less amount of water provided the best heat propagation (Comina et al., 2013).
- When a water inflow was afforded, the advection played the major role in transporting the heat through the porous medium. The advective phenomenon improves significantly the heat propagation, resulting in an increase of the effective thermal conductivity (Comina et al., 2013).
- After the source's turn off, the cool down is more rapid in high water content conditions and even higher when a water flow is induced. A BTES plant has to reach a compromise between the heat injection and the heat losses. The unsaturated zone of an aquifer could therefore favorable be exploited, being the potential heat losses lower than below the water table.

3.3 Numerical Simulations and Geophysical Monitoring: Results and Discussion

Several tests were performed on different media at different conditions (Firmbach et al., 2013; Giordano et al., 2013a, Giordano et al., 2013b). The results here presented refer to the condition at $\theta = 100$ % vol. with no water flow. The numerical simulation carried

out with OpenGeoSys was calibrated with the temperature recordings at each T-sensor located in the box (Figure 4a). The numerical output provided a reliable interpolation of the temperature distribution within the medium and this was adopted to evaluate the goodness of the electrical resistivity monitoring. The best fit between experimental and resistivity-derived temperatures was achieved with a fractional change $m = 0.021 \text{ } ^\circ\text{C}^{-1}$ (Figure 4b).

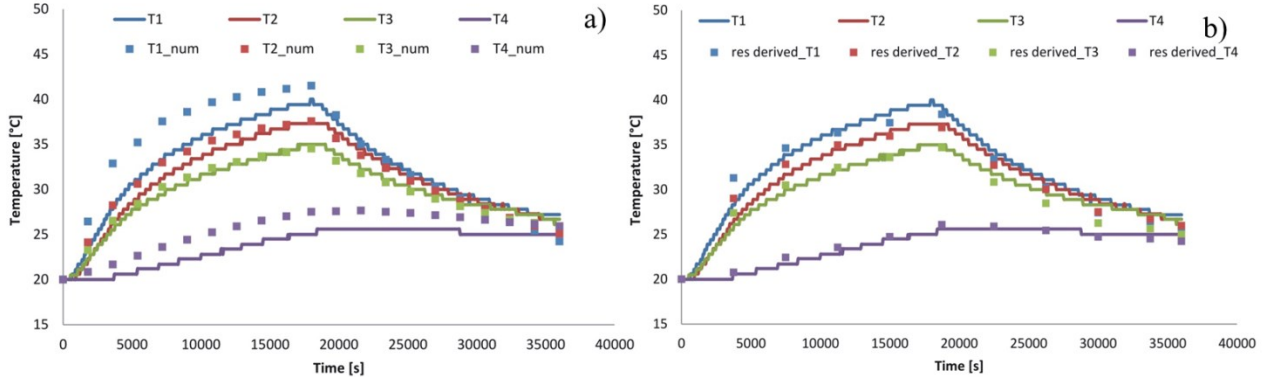


Figure 4: a) Comparison between experimental and numerically modelled temperature. b) Comparison between experimental and resistivity-derived temperature.

The resistivity-derived temperatures were also drawn in a 2D representation obtained with a Kriging interpolation of the various measurements within the box (Figure 5). The heating period is in valid accordance with the peak temperatures and the shape of the heated plume. The cool down is also correctly described by the resistivity monitoring. The geoelectric surveying validly described the TAZ induced in the medium during the heat injection and the little overestimation of their extension can be seen as conservative. It highlighted its potentiality in describing the heat diffusion from the source in all the tests.

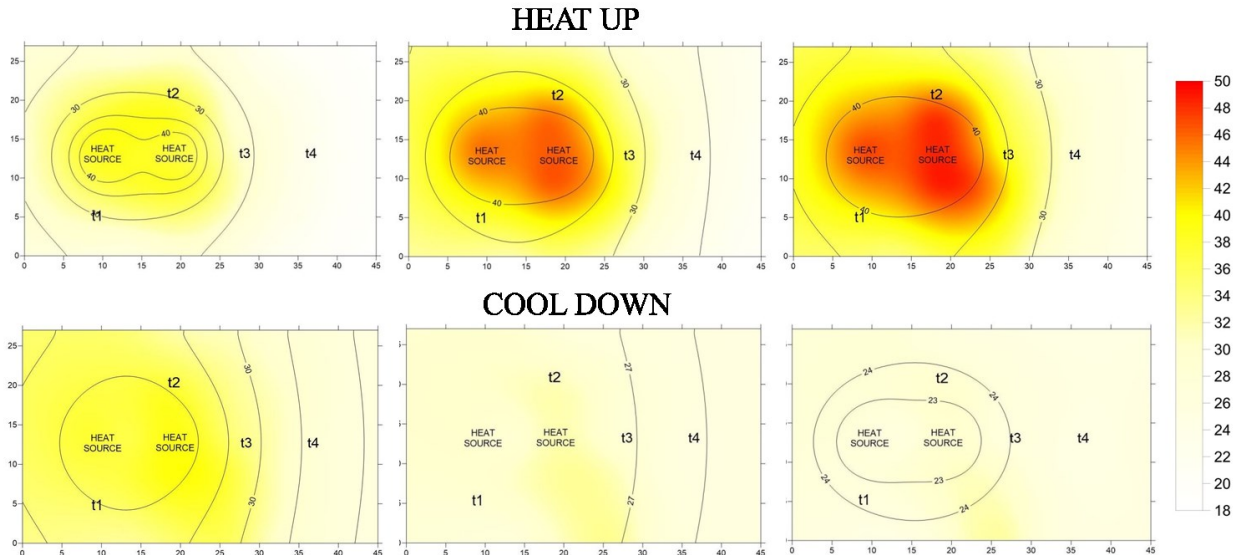


Figure 5: Comparison between electrical resistivity monitoring (colors map) and numerical simulation with OpenGeoSys (contour map). The maps refer to 1, 3, 5, 6, 8 and 10 h from the beginning of the test.

4. FIELD SCALE

4.1 Materials and Methods

4.1.1 The Grugliasco Test Site

A BTES living lab has been built in Grugliasco (Torino, Italy) in the campus of the *Scuola di Agraria e Medicina Veterinaria* of the Torino University. The test site is situated in the north-western portion of the Pianura Padana, between the Sangone River on the South, the Po River on the East and the Dora Riparia River on the North. Here, abundant Pleistocene-Holocene glacio-fluvial coalescing fans are connected with the alluvial plain of the Po River, which on turn lays on the Torino Hill lithological units (Figure 6). The deposits therefore mainly consist of gravelly sandy materials with high permeability and they host a phreatic aquifer in the first 50-60 m below the ground, in which the groundwater flows eastward directly connected with the Po River. The water table in the Grugliasco area lays 30-40 m below the ground level. Owing to administrative regulations and in order to test the ability of dry alluvial deposits in storing the heat, as depicted from the above presented laboratory tests, the plant was decided to be hosted in the unsaturated zone of the unconfined aquifer. The system (Figure 7) consists in capturing solar energy by means of 2 solar thermal panels (Vitosol 200-F, Viessmann) and storing the heat in the ground by four 27 m deep BHEs (pipes GEROtherm PE100-RT, grout Termoplast - Laviosa Chimica Mineraria Spa). An electrical hydraulic pump of 59 W (Stratos ECO 25/1-5 BMS - WILO) provides the thermo-vector fluid circulation through the whole system at 200 l/h flow rate and 2.2 bar constant pressure (the chosen anti-freeze additive is Propylene Glycol at 40% vol. concentration). A double-U piped borehole is placed in the center of an equilateral triangle (2 m side), and the other 3 single-U piped boreholes are located to the triangle's vertexes. A 33 m deep

piezometer is located 2 m away from the double-U heat exchanger for monitoring the potentiometric surface oscillations. The thermo-vector fluid, warmed by solar energy, is driven down into the central BHE, then out to the hydraulic pump and re-pumped down into the external BHEs afterwards. Such a circulation is supposed to simulate what really happens in the BTES systems, where a core volume benefits from the hottest carrier fluid and an annular volume is powered by heat-waste only. A total of 20 RTD 4wire pt100 (accuracy 5%, resolution 0.01°C) are placed every 5 m down-hole in the 3 BHEs and in the piezometer. In addition, 10 temperature sensors of the same type are placed throughout the whole circuit and in the thermal panels. All the sensors are connected to a CentralLine Honeywell data logger which continuously collects the data, providing a 0.5 h sample interval. All the plant is managed in remote control from the Earth Science Department in Torino. After preliminary tests in fall 2013, the system was launched in March 2014 and the temperature monitoring started on the 2nd of April 2014. Some direct measurements of the thermal conductivity of the involved geological materials and the geothermal grout were also carried out, in order to define detailed input values for the numerical model.

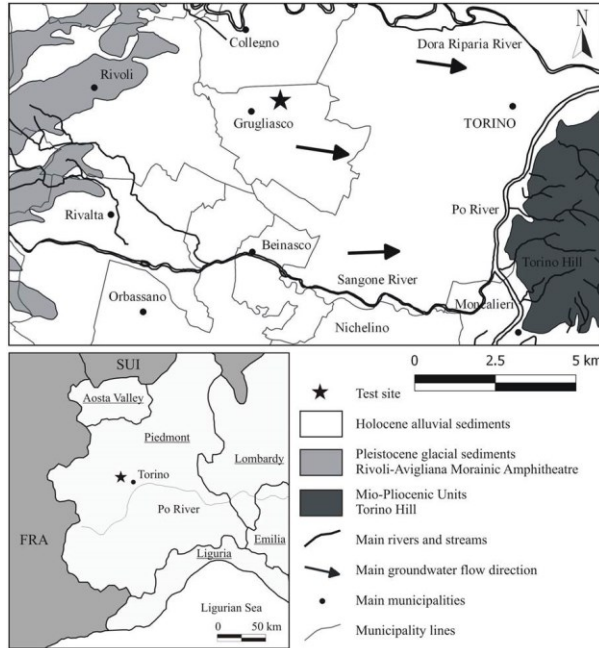


Figure 6: Geographical and geological test site location.

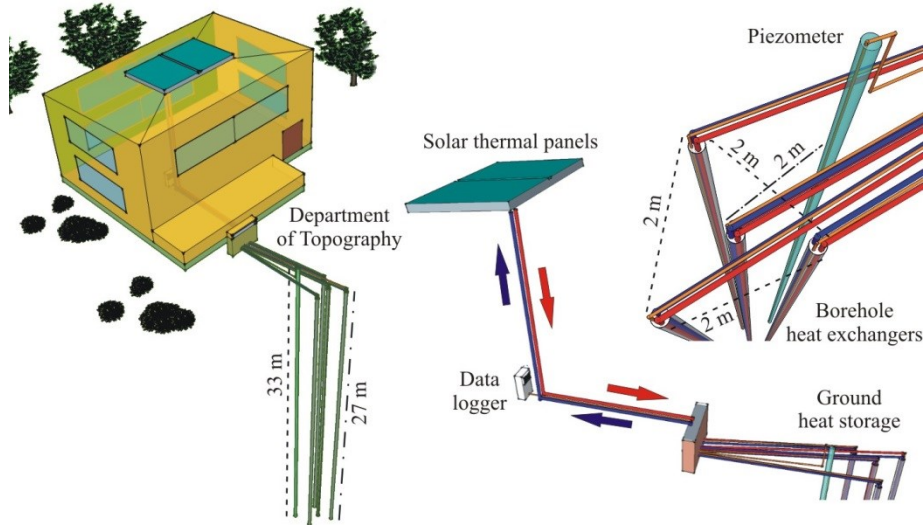


Figure 7: Sketch of the Grugliasco BTES pilot plant.

4.1.2 Numerical simulations

A 3D quadrilateral 50x50x30 m model of the Grugliasco site was developed and OpenGeoSys was adopted as in the lab scale modeling. A triangular prismatic mesh of about 120,000 nodes was adopted; the mesh is finer in the centre of the model and progressively coarser in the further portions. The model was chosen wide enough so that the lateral boundary conditions do not influence the simulation's output. The adopted physical properties of the ground are presented in Table 3. The borehole heat exchangers were simulated as linear elements surrounded by geothermal grout for a diameter of 0.15 m. The system was simulated for 5 years by featuring an alternation between heat injection and extraction of 6 months. During the warm season each day should be simulated by an injection at about 60 °C for 8 h and at 30 °C for the remaining 16 h (Diersch et al., 2011), nevertheless this kind of discretization would need excessive computation time. In order to speed up the simulation, a weighted average inlet temperature was therefore chosen: 40 °C in the central BHE and 30 °C in the externals. During the winter period, an inlet constant temperature

of 10 °C was adopted. The whole simulation time was discretized in 365 steps of 5 days each one. The simulations were performed on a computer equipped with an Intel® Core™ i5-3317U 1.70 GHz CPU processor with 4.00 GB of RAM and the 64-bit Microsoft Windows 8® operating system.

Numerical model properties

Undisturbed T [°C]	14.5
Porosity	0.3
Water content [%]	40
Volumetric heat capacity [MJ m ⁻³ K ⁻¹]	2.3
Thermal conductivity [W m ⁻¹ K ⁻¹]	1.7
Grout thermal conductivity [W m ⁻¹ K ⁻¹]	1.0

Table 3: Model properties adopted in the OGS 3D simulation of the Grugliasco site.

4.1.3 Geophysical surveys

Many different electrode configurations were tested. Owing to the limited dimensions of the area around the BHEs system, it was decided to perform (i) a Wenner-Schlumberger linear acquisition with 1 m spaced 72 electrodes and (ii) a quasi-3D Dipole-Dipole acquisition with 72 electrodes arranged in a 3 m spaced 9x8 grid (Figure 8). A SYSCAL Pro multichannel georesistivimeter was also used for resistivity field measurements. The first configuration allows us to image the thermal influence up to about 15 m below the ground level, while the second, reaching a depth of investigation of 5-6 m only, can however provide a plan view just around the heat injection source, as the laboratory measurements afforded. The surveys have been performed monthly from the startup of the plant (zero condition) in order to apply the same methodology calibrated at lab scale (Equation [6]).

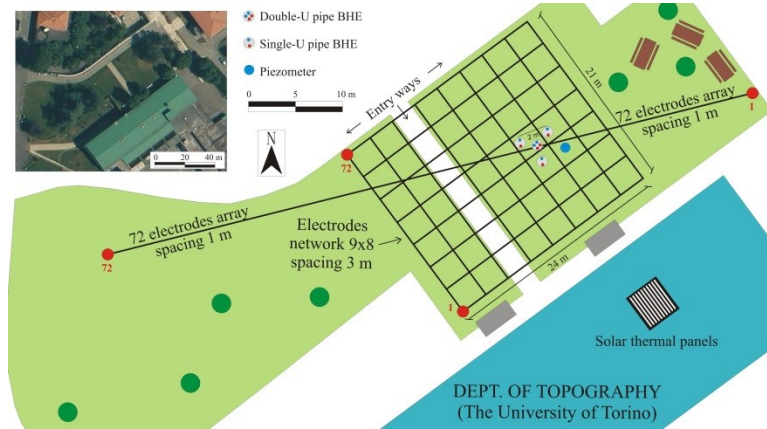


Figure 8: Location of the geophysical surveys in the Grugliasco site.

4.2 Temperature Monitoring: Results and Discussion

Generally there was a calm weather in April 2014 in Grugliasco and an overall positive trend was therefore monitored in the ground's temperature. Nevertheless, two critical periods can be pointed out. From 18/04 to 19/04 and from 27/05 to 02/05 a bad turn in the weather was observed and the ground's temperature recorded two negative trends, the latter more pronounced owing to the longer duration of bad weather. Figure 9 shows how the air temperature and the solar radiation influenced the temperature of the thermal panels. In rainy days, if the air temperature was high the thermal panels managed to reach rather large temperature values anyway. In sunny days, when the solar radiation was around a thousand W m⁻², the air temperature also seemed to influence the thermal panels' activity.

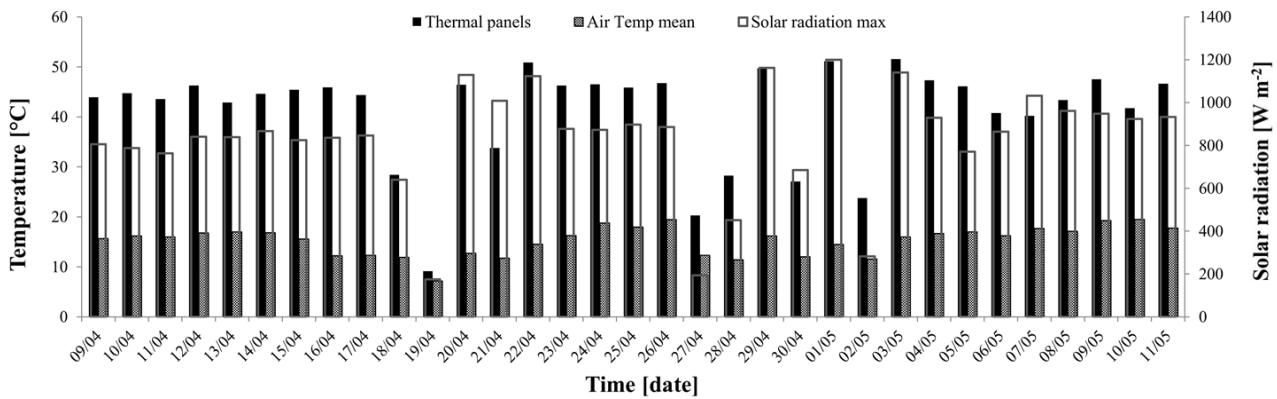


Figure 9: Comparison among the temperature provided by thermal panels, the mean air temperature and the maximum solar radiation (climatic data provided by two weather stations located in Torino and Grugliasco).

The first month of temperature monitoring showed a day-night alternation more emphasized in the central BHE (Figure 10), where the thermo-vector fluid passes through it at the maximum temperature reached in the thermal panels. The maximum daily ΔT between the central and external BHEs was around $3.5 - 4$ °C and it happened in the middle of the afternoon (about 3 – 4 PM). The maximum temperature in the thermal panels was recorded between noon and 1.30 PM, while in the central BHE was observed a couple of hours later in time; in the externals the peaks happened always in the late afternoon as well.

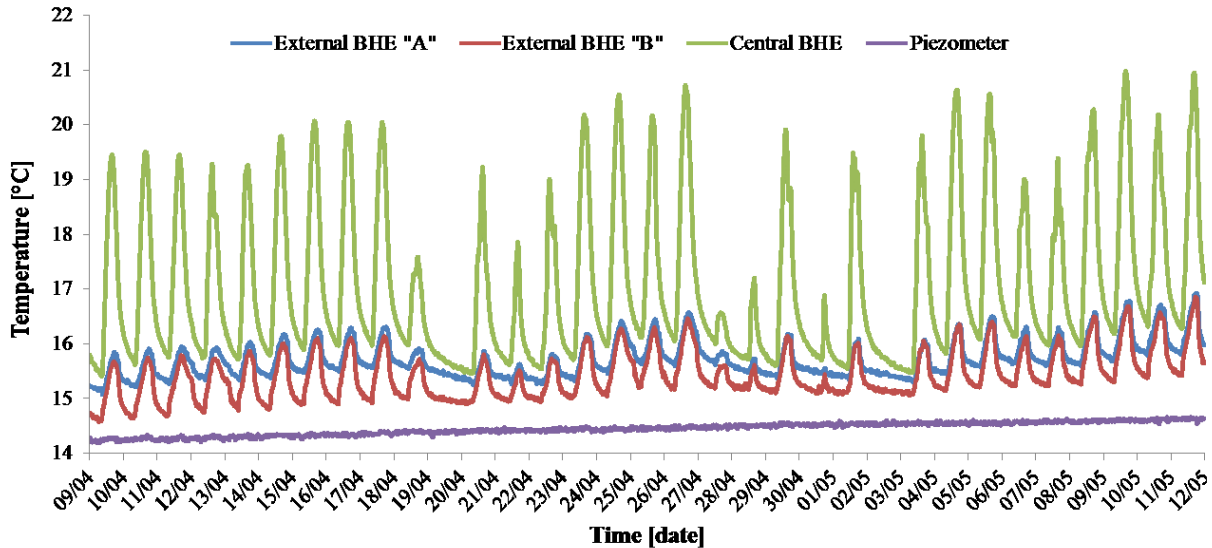


Figure 10: Temperature observations in the first operative month of the plant.

4.3 Numerical Simulations: Results and Discussion

The numerical simulations managed to render reliable and close-to-reality results and the 5 year simulation gave the chance to make interesting considerations (Figure 11). The 6 month alternation between heat injection and extraction would provide a general equilibrium temperature within the ground. The involved temperatures (40 and 30 °C during the injection and 10 °C during the extraction) would generate a cool down of the ground after the first year of operation: a decrease from the undisturbed 14.5 °C to about 14 °C was rendered outside the borehole field. Nevertheless, a general increasing trend of the minimum ground temperature is clear during the 5 years of simulation. The temperatures close to the boreholes are strictly related to the temperature of the refrigerant circulating in the pipes, while the control points in the piezometer showed a better thermal inertia and thus a higher heat storage capacity.

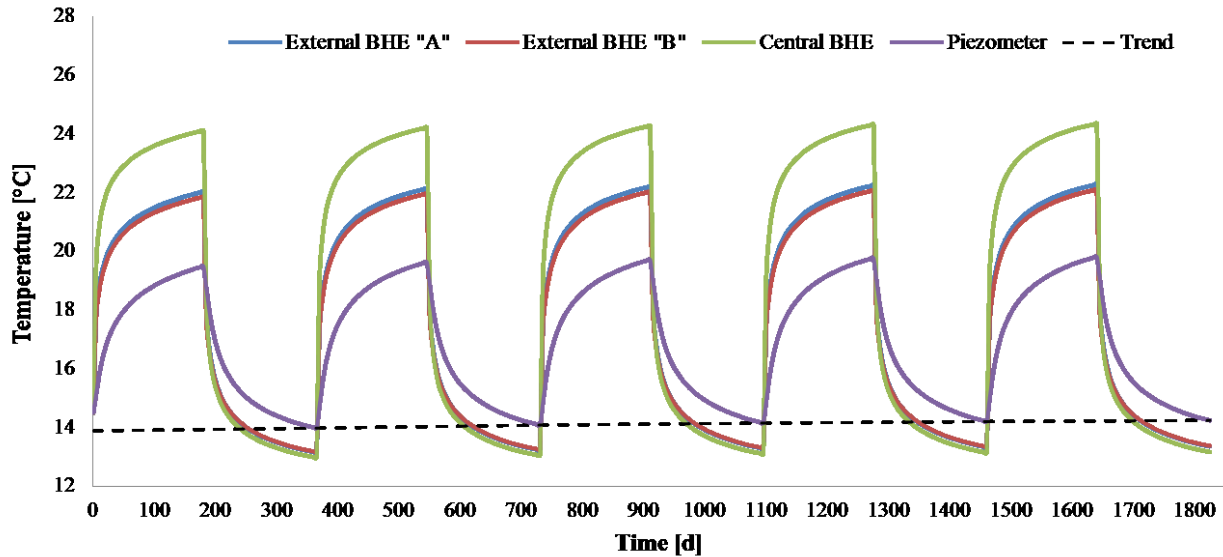


Figure 11: Temperature prediction in the BHEs and the piezometer during the next 5 years.

The evaluation of the thermal influence after 4.5 years from the start up (after the last heat injection period) showed the isotherm 17.5 °C (+3 °C from undisturbed T) having a 5.4 m radius, while an increase of 1 °C was simulated to have a 15.1 m radius (Figure 12). Table 4 shows the daily temperature fractional changes registered by the Grugliasco BHEs in the first operative month compared with the numerical results at the end of the first heat injection period (about 180 days). The predictions rendered that the central heat exchanger will maintain the current temperature growth, while the external BHEs and the piezometer will increase in the next months. Obviously the first month was far from being a typical injection period as that simulated with OpenGeoSys. Hence, more time is needed to find agreement in this direction.

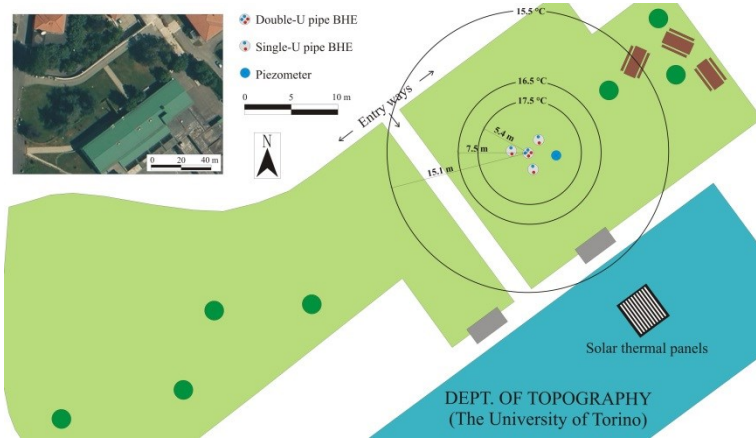


Figure 12: Thermal affected zone deduced by numerical simulation at 4.5 years from the start up.

<i>Slope coefficient [°C⁻¹]</i>	<i>Field</i>	<i>Numeric</i>
External BHE 'A"	0.0581	0.0685
External BHE 'B"	0.0467	0.0639
Central BHE	0.1178	0.0967
Piezometer	0.0141	0.0441

Table 4: Slope coefficients of the temperature regression curves registered by the Pt-100s compared with those rendered by the OpenGeoSys control points.

5. CONCLUSIONS

A multidisciplinary approach for evaluating the thermal behavior of a sandy gravelly ground subjected to heat injection was first applied and calibrated at laboratory scale and then carried out in the first operative month of the BTES living lab built in Grugliasco (Torino, Italy). The methodology encompasses temperature monitoring, numerical modeling and geophysical surveying in synergy for understanding the differences in heat propagation within a porous medium at changing water content and with advective flow as well. A qualitative and quantitative description of the TAZ induced in a porous medium was successfully performed at lab scale. The same methodology is being applied at field scale: the temperature monitoring and thermal property assessment already gave valid outcomes, helpful for the construction of a reliable numerical model. The geophysical surveying provided the zero condition and did not highlight a significant thermal influence in the first month. Further temperature monitoring and geophysical measurements are needed to assess the ground's thermal behavior.

These are of course preliminary tests of a work in progress living lab, oriented to understand the system's characteristics, the functionality of the remote control and the different operating conditions of the coupled thermal panels and BHEs arrangement. This kind of system needs several months to work at operating speed and a number of tests for its optimization. The numerical simulation coupled with the field temperature monitoring is a fundamental tool for minimizing the unknowns and for predicting the thermal behavior of the ground subjected to the heat injection. In parallel, the application of a geophysical surveying such as the one proposed can help in the calibration of an indirect methodology, helpful in different situation where direct measurements are not available.

ACKNOWLEDGMENTS

The living lab in Grugliasco was designed by Ing. Andrea Cagni (EQ Ingegneria, Busca, Cuneo, Italy) and built by Somiter Srl (Saluzzo, Cuneo, Italy) under the supervision of Geol. Maurizio Colla. The funding for the experimental site were provided by EU Alcotra Innovation 2012 and P.O.R. - F.E.S.R. 2013: projects which aim for pilot actions of lab and field testing of heat storage applications and knowledge spreading with living lab approach. The authors would like moreover to acknowledge Dr. Antonio Galgaro and Dr. Eloisa Di Sipio for performing the thermal property analysis with the device ISOMET 2114 at the Department of Geoscience of the University of Padova.

REFERENCES

Abu-Hamdeh, N.H. and Reeder, R.C.: Soil Thermal Conductivity: Effects of Density, Moisture, Salt Concentration and Organic Matter, *Soil Science Society American Journal*, **64**, (2000), 1285-1290.

Anderson, M.P.: Heat as a Ground Water Tracer, *Ground Water*, **43**(6), (2005), 951-968.

Arslan, U. and Huber, H.: Numerical Back-Analyses of Laboratory Tests With Forced Groundwater Flow, *Proceedings*, 38th Workshop on Geothermal Reservoir Engineering, (2013), 1-5.

Bonte, M.: Impacts of Shallow Geothermal Energy on Groundwater Quality: A Hydrochemical and Geomicrobial Study of the Effects of Ground Source Heat Pumps and Aquifer Thermal Energy Storage, *Phd Thesis*, Gildeprint Enschede, ISBN 978-94-6108-544-3, (2013), 175 pp.

Campbell, G.S. and Norman, J.M.: An Introduction to Environmental Biophysics, *Springer-Verlag*, New York, (1998), 291 pp.

Chen, S.X.: Thermal Conductivity of Sands, *Heat Mass Transfer*, **44**, (2008), 1241-1246.

Comina, C., Dietrich, P., Firmbach, L., Giordano, N., Kolditz, O., Mandrone, G., Vienken, T. and Watanabe, N.: Heat Flow's Propagation Within a Porous Medium: Analogical and Numerical Modeling. *Proceedings*, European Geothermal Congress, ISBN 978-2-8052-0226-1, (2013), 1-8.

Dickinson, J.S., Buik, N., Matthews, M.C. and Snijders, A.: Aquifer Thermal Energy Storage: Theoretical and Operational Analysis, *Geotechnique*, **59**, (2009), 249-260.

Diersch, H.J.G., Bauer, D., Heidemann, W., Rühaak, W. and Schätzl, P.: Finite Element Modeling of Borehole Heat Exchanger Systems: Part 2 Numerical Simulation, *Computers & Geosciences*, **37**, (2011), 1136-1147.

Farouki, O.T.: Thermal Properties of Soils, *CRREL Monograph*, 81-1, US Army Corps of Engineers, Cold Regions Research and Engineering Laboratory, Hanover, NH, (1981), 136 pp.

Firmbach, L., Giordano, N., Comina, C., Mandrone, G., Kolditz, O., Vienken, T. and Dietrich, P.: Experimental Heat Flow Propagation within Porous Media Using Electrical Resistivity Tomography (ERT), *Proceedings*, European Geothermal Congress, ISBN 978-2-8052-0226-1, (2013), 1-7.

Fisch, M.N., Guigas, M. and Dalenbäck, J.O.: A Review of Large-Scale Solar Heating Systems in Europe, *Solar Energy*, **63**(6), (1998), 355-366.

Fragkogiannis, G., Papatheodorou, N. and Stamataki, S.: Evaluation of Thermal Performance of Ground - Source Energy Systems. A Geophysics Supported Approach, *Proceedings*, X World Renewable Energy Congress and Exhibition, Glasgow, Scotland, (2008).

Friedman, S.P.: Soil Properties Influencing Apparent Electrical Conductivity: a Review, *Computers and Electronics in Agriculture*, **46**, (2005), 45-70.

Giordano, N., Bima, E., Caviglia, C., Comina, C., Mandrone, G. and Passarella, M.: Modellizzazione Analogica e Numerica di un Flusso Termico in un Mezzo Poroso in Laboratorio Attraverso Scatola Termica, *Geoingegneria Ambientale e Mineraria*, **3**, (2013) 49-62.

Giordano, N., Firmbach, L., Comina, C., Dietrich, P., Mandrone, G. and Vienken, T.: Laboratory Scale Electrical Resistivity Measurements to Monitor the Heat Propagation within Porous Media for Low Enthalpy Geothermal Applications, *Proceedings*, 32° Convegno Nazionale del GNGTS, ISBN 978-88-902101-8-1, (2013), 122-128.

Hayashi, M.: Temperature-Electrical Conductivity Relation of Water for Environmental Monitoring and Geophysical Data Inversion, *Environmental Monitoring and Assessment*, **96**, (2004), 119-128.

Hayley, K., Bentley, L.R., Gharibi, M. and Nightingale, M.: Low Temperature Dependence of Electrical Resistivity: Implications for Near Surface Geophysical Monitoring, *Geophysical Research Letters*, **34**, (2007), L18402.

Hecht-Méndez, J., Molina-Giraldo, N., Blum, P. and Bayer P.: Evaluating MT3DMS for Heat Transport Simulation of Closed Geothermal Systems, *Ground Water*, **48**(5), (2010), 741-756.

Hermans, T., Vandenbohede, A., Lebbe, L., Nguyen, F.: A Shallow Geothermal Experiment in a Sandy Aquifer Monitored Using Electric Resistivity Tomography, *Geophysics*, **77**(1), (2012), B11-B21.

Kolditz, O., Bauer, S., Bilke, L., Böttcher, N., Delfs, J.O., Fischer, T., Görke, U.J., Kalbacher, T., Kosakowski, G., McDermott, C.I., Park, C.H., Radu, F., Rink, K., Shao, H.B., Sun, F., Sun, Y.Y., Singh, A.K., Taron, J., Walther, M., Wang, W., Watanabe, N., Wu, Y., Xie, M., Xu, W. and Zehner, B.: OpenGeoSys: an Open-source Initiative for Numerical Simulation of Thermo-Hydro-Mechanical/Chemical (THM/C) Processes in Porous media, *Environmental Earth Science*, **67**, (2012), 589-599.

Lo Russo, S., Gnavi, L., Roccia, E., Taddia, G. and Verda, V.: Groundwater Heat Pump (GWHP) System Modeling and Thermal Affected Zone (TAZ) Prediction Reliability: Influence of Temporal Variations in Flow Discharge and Injection Temperature, *Geothermics*, **51**, (2014), 103-112.

Novo, A.V., Bayon, J.R., Castro-Fresno, D. and Rodriguez-Hernandez, J.: Review of Seasonal Heat Storage in Large Basins: Water Tanks and Gravel-Water Pits, *Applied Energy*, **87**, (2010), 390-397.

Ochsner, T.E., Horton, R. and Ren, T.: A New Perspective on Soil Thermal Properties, *Soil Science Society American Journal*, **65**, (2001), 1641-1647.

Paskoy, H.O., Andersson O., Abaci, S., Evliya, H. and Turgut, B.: Heating and Cooling of a Hospital Using Solar Energy Coupled with Seasonal Thermal Energy Storage in an Aquifer, *Renewable Energy*, **19**, (2000), 117-122.

Reuss, M., Beuth, W., Schmidt, M. and Schoelkopf, W.: Solar District Heating with Seasonal Storage in Attenkirchen, *ECOSTOCK 2006*, in: 10th International Conference on Thermal Energy Storage, Stockton, USA, (2006).

Revil, A., Cathles, L.M., Losh, S. and Nunn, J.A.: Electrical Conductivity in Shaly Sands with Geophysical Applications, *Journal of Geophysical Research*, **103**, (1998), 23925-23936.

Robert, T., Hermans, T., Dumont, G., Nguyen, F. and Rwabuhungu, D.E.: Reliability of ERT-Derived Temperature – Insights from Laboratory Measurements. *Proceedings*, 19th European Meeting of Environmental and Engineering Geophysics, (2013), TuS2a10.

Sanner, B., Karytsas, C., Mendlinos, D. and Rybach, L.: Current Status of Ground Source Heat Pumps and Underground Thermal Energy Storage in Europe, *Geothermics*, **32**, (2003), 579-588.

Schmidt, T., Mangold, D. and Müller-Steinhagen, H.: Central Solar Heating Plants With Seasonal Storage in Germany, *Solar Energy*, **76**, (2004), 165-74.

Tarnawski, V.R. and Leong, W.H.: Thermal Conductivity of Soils at Very Low Moisture Content and Moderate Temperatures, *Transport in Porous Media*, **41**, (2000), 137-147.

WEB REFERENCES

DLSC – Drake Landing Solar Community, 2012. Borehole thermal energy storage (BTES), available from: <http://dlsc.ca>.

Solar radiation data – Weather station to the UNITO Department of Physics, Torino, available from <http://www.meteo.dfg.unito.it/home>.

Temperature data – Weather station to the UNITO Department of Agricultural, Forest and Food Sciences, Grugliasco, available from http://87.241.36.75:8080/gpmeteo/index.jsp?rete=RAM_UTENTI&g=null.

Xu, J., Wang, R.Z. and Li, Y.: A Review of Available Technologies for Seasonal Thermal Energy Storage, *Solar Energy*, (2013), available from <http://dx.doi.org/10.1016/j.solener.2013.06.006>.